Semiconductor Nanowire Ring Resonator Laser

Peter J. Pauzauskie,[1,2] Donald J. Sirbuly,[1,2] and Peidong Yang[1,2,*]

[1]*Department of Chemistry, University of California at Berkeley, Berkeley, California 94720, USA*
[2]*Materials Sciences Division, Lawrence Berkeley National Laboratory, Berkeley, California 94720, USA*

(Received 28 January 2006; published 13 April 2006)

Nanowires of the wide band-gap semiconductor gallium nitride (GaN) have been shown to act as room-temperature uv lasers. Recent advances in nanomanipulation have made it possible to modify the shape of these structures from a linear to a pseudoring conformation. Changes to the optical boundary conditions of the lasing cavity affect the structure's photoluminescence, photon confinement, and lasing as a function of ring diameter. For a given cavity, ring-mode redshifting is observed to increase with decreasing ring diameter. Significant shifts, up to 10 nm for peak emission values, are observed during optical pumping of a ring resonator nanolaser compared to its linear counterpart. The shifting appears to result from conformational changes of the cavity rather than effects such as band-gap renormalization, allowing the mode spacing and position to be tuned with the same nanowire gain medium.

DOI: 10.1103/PhysRevLett.96.143903 PACS numbers: 42.55.Sa, 42.25.Gy, 42.60.Da, 78.67.Lt

Recently, semiconductor nanowires have gained considerable attention as components in future integrated optical systems due to their multifunctional behavior as active gain media, passive waveguides, and evanescent-field chemical sensors [1]. As a result of their dimensionality, crystalline structure, and composition, low dimensional nanomaterials offer a unique platform to study effects such as electron, phonon, and photon confinement as well as mechanical properties. This study focuses on the wide band-gap semiconductor GaN which is currently a candidate for future short-wavelength, high-power, and high-temperature optoelectronic devices. One-dimensional nanostructures made of single-crystalline GaN, which now include nanowires [2,3], nanotubes [4], and core-sheath structures [5], already show great promise as nanometer light sources and subwavelength photonic components [6].

The theory of electromagnetic modes and gain in nanowire cavities has been developed significantly in the last several years, helping to illuminate how the diffraction-limited cavity-apertures affect nanowire lasing. Recent theoretical work on vertical, freestanding nanowires has shown how end-facet reflectivities, modal gain, and lasing depend heavily on mode type, cavity size, and the gain medium [7,8]. Other novel optical microcavity effects [9] that hold both fundamental and applied interests include amplified or inhibited spontaneous emission rates (Purcell effect), single photon emission, low threshold lasing, and photonic-molecule cavities [10]. Semiconductor microcavities provide a fertile testing ground for experimental quantum electrodynamics, as well as light-based information processing [11–13]. Recent advances in cavity manipulation have enabled the physical restructuring of nanowires into arbitrary geometries. Here we report on a new structural geometry, a nanowire-ring laser, which shows markedly different lasing and spontaneous emission properties compared to its linear counterpart.

Synthesis and Construction of Rings.—GaN nanowires were synthesized via a chemical vapor transport process in a hot-wall furnace at 900 °C with metallic gallium and ammonia precursors [1]. Single $[1\bar{1}0]$ growth-direction wires with triangular cross sections were cut with a micropositioning system [Fig. 1(a)] and placed on a silicon wafer with a 100 μm thermal oxide layer. The ring structures were fashioned with the micromanipulator by pushing the two ends together in a side-by-side geometry to ensure optical coupling [14].

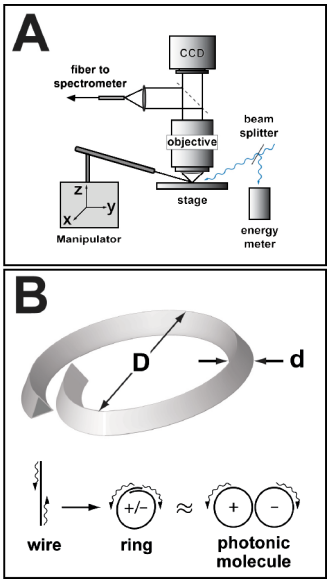

FIG. 1 (color online). (a) Schematic of the instrumental setup for nanowire manipulation and lasing experiments. (b) Schematic of ring structures showing the triangular cross section of the nanowires, and the side-by-side overlap that enables evanescent coupling between cavity arms. The circulating optical modes within a resonator cavity containing a defect are theoretically equivalent to a photonic molecule.

Wires were manipulated with the probe under a dark-field microscope equipped with a 50× objective (0.55 NA). A HeCd laser provided ~5 mW of unpolarized continuous wave (cw) excitation at 325 nm, while the 4th harmonic of a Nd:YAG laser (266 nm, 8 ns, 10 Hz) was used for optical pumping. The laser was focused to a beam diameter of ~50 μm, giving a HeCd-cw power density of 175 W/cm^2 and a YAG pulsed energy density of 1–1000 μJ/cm^2. Spectra were acquired with a fiber coupled to a spectrometer (1200 grooves/mm grating) and liquid-N_2 cooled CCD. Unless specified otherwise, fifty 0.1 s exposures were accumulated for a given spectrum, roughly corresponding to 50 pulse events. The pulse energies were measured and averaged using an energy detector-meter pair. Grey-scale and color images were recorded with separate microscope-mounted CCD cameras.

Boundary Conditions.—A crucial physical difference between linear and ring cavity geometries is that the ring resonator case requires phase matching at the end-facet junction, forcing integer-wavelength boundary conditions for gain within the cavity. Therefore, the spacing of modes within the cavity is given approximately by the well-known expression:

$$\Delta\lambda = \frac{\lambda_0^2}{2\pi R(n - \lambda_0 \frac{dn}{d\lambda}|_{\lambda_0})}. \quad (1)$$

The expression is approximate because the effect of the substrate dielectric on phase dispersion is neglected. In contrast, linear nanowire lasers act as Fabrey-Perot (FP) cavities with boundary conditions that require integer numbers of half-wavelength standing waves. Also, both the substrate dielectric and the triangular symmetry of the nanowire's cross section break the azimuthal symmetry of the cavity, eliminating the possibility of separate TE or TM modes [15] which are fundamental in models of freestanding cavities.

Photoluminescence (PL).—There is a clear change in the PL of the ring structure as compared to the nanowires, particularly in the emergence of modulation on the red side of the spontaneous emission band [Fig. 2(c)]. Modes do not occur on the blue side of the PL band because of near-band-edge photon reabsorption. The mode spacings calculated for these peaks in Eq. (1) correlate well with those expected for a circular resonator: 1.4 nm splitting for an 8 μm ring at 380 nm modal wavelength, where the measured value [Fig. 2(d)] is 1.2 nm. Interestingly, the individual modes on the red half of the spontaneous emission band split further into doublets [$\Delta\lambda|_{400\ \mathrm{nm}} \sim 0.5$ nm, Fig. 2(c), inset]. Because of the dielectric discontinuity after coupling [Fig. 1(b)], an unavoidable perturbation is introduced within the cavity, breaking the resonance's degeneracy into clockwise and counterclockwise mode propagation. Mode degeneracy has been shown to split due to random imperfections in the cavity such as root-mean-square surface roughness [16] or from intentionally placed dielectric discontinuities within [17] or attached to [18] the resonant cavity. All three kinds of perturbation exist within these physically shaped nanowire-ring resonators. It has been shown that a perturbed cavity is theoretically equivalent [17] to two perfect cavities that are coupled, such as with a photonic molecule [see Fig. 1(b)] [10]. This leads to degeneracy splitting into "bonding" and "antibonding" modes, using a molecular analogy.

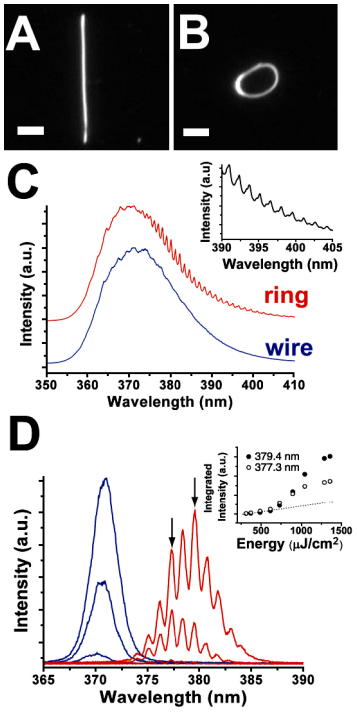

FIG. 2 (color online). (a) A linear gallium nitride nanowire before physical manipulation of it into a ring configuration; scale bar = 5 μm. (b) Corresponding ring geometry made from the wire in (a); scale bar = 5 μm. (c) Photoluminescence spectra corresponding to the wire and ring configurations. Inset: Expansion of ring's higher-wavelength region with pronounced mode splitting. (d) Lasing spectra for the wire [dark (blue online)] and ring [light (red online)] structures. Maximum plotted emission for each structure was taken at the same excitation intensity of 1050 μJ/cm^2. Arrows correspond to integrated modes within the inset. Inset: Modal gain analysis for two separate modes from the ring resonator cavity.

Lasing.—The lasing behavior between nanowires and their resonator counterpart is also markedly different. The ring lasing-emission maximum redshifts substantially, in some cases by as much as 10 nm [Fig. 2(d)], relative to the wire. For example, under similar power fluences (1050 μJ/cm^2), the ring laser in Fig. 2(d) has its maximum emission intensity 9 nm red shifted in comparison to the linear structure. Though an electron-hole plasma (EHP) is the likely lasing mechanism for both the wire and ring [3], the redshift cannot be explained by a simple wire heating or band-gap renormalization argument due to the size of the shift. Further analysis of the pronounced shift will be discussed in more detail below. Integration of individual ring-mode intensities at 377.3 and 379.4 nm shows characteristic gain pinning [Fig. 2(d), inset]. Also, the redshift in the ring-mode spectral center as a function of increasing

pump fluences [Fig. 4(c), ring, 376.4 nm] is consistent with EHP dynamics. The absence of laser mode splitting in Fig. 2(d) relates to enhanced scattering of shorter wavelengths, and is discussed further below. Far-field emission images [Fig. 3(b)] collected from a single ring resonator clearly show distinct interference patterns, indicating that light scattered from end facets is highly coherent.

Weakly coupled cavities displayed both linear (FP) modes and higher-spaced ring resonator modes as seen in Fig. 3(c). An electron micrograph of one such cavity [Fig. 3(c), inset] reveals different air-gap distances of 20 nm (top) and 95 nm (bottom) on opposite ends of the junction. Presumably this partial breakage of the coupling allows amplification of both the ring and FP modes. The measured mode spacing values in Fig. 3(c) are 1.61 nm at 377 nm (ring) and 0.69 nm at 375 nm (wire), leading to a ring/wire mode spacing ratio of 2.34. Using a Sellmeier dispersion [19] the calculated value for this ratio, $\Delta\lambda|_{\mathrm{ring,377\ nm}}/\Delta\lambda|_{\mathrm{wire,375\ nm}}$, is 2.32, indicating that both FP and ring modes experience gain. Lastly, after comparing with the PL spectra, lasing occurs preferentially in the red member of the ring-mode doublet [Fig. 3(c), lighter lines (red online)], most likely due to increased isotropic scattering of the shorter wavelengths [17].

Measured thresholds of wire and ring structure are comparable, with wire lasing-onsets near 75 μJ/cm^2, while typical ring onsets appear to increase by ~50%. The wire threshold is consistent with previously reported values using nanosecond pump pulses at 4.66 eV (266 nm) [1]. However, since planar ring structures exhibit a significant amount of in-plane lasing [20], comparison of wire and ring lasing threshold are questionable with the far-field collection geometry of this work. More sensitive measurements that could be employed include near-field probes or tangential-fiber output coupling. Alternatively, it is experimentally possible to measure differences in photon confinement through comparison of cavity quality (Q) factors. Cavity Q factors were measured from wire and ring lasing-emission spectra [Fig. 3(d)] following single-pulse excitation of the cavity shown in Fig. 4(c). When the cavity is coupled to form a ring, quality factors ($Q = \lambda/\Delta\lambda = 2\pi\nu t_c$, t_c = phonon confinement time) are measured to be higher than 10^3, which is approximately an order of magnitude larger than what is predicted for freestanding wires with diffraction-limited reflectivities [21], but comparable to what has been observed in linear GaN cavities [3,22]. After the ring is decoupled there is an increase of the modal FWHM by ~0.2 nm, corresponding to a 40% drop in the cavity's Q factor due to a decrease in the photon-confinement lifetime.

The flexibility and strength of the GaN nanowires allows for the cutting and reforming of ring structures with progressively smaller diameters while keeping the cavity diameter constant. Figure 4 illustrates one such ring which starts with a diameter of ~16 μm. Lasing and PL spectra were then captured for each coupled and uncoupled cavity

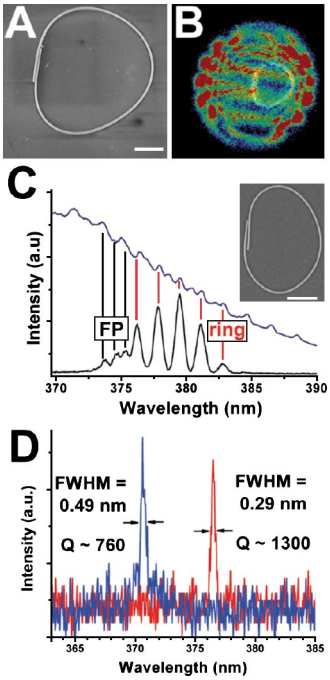

FIG. 3 (color online). (a) Scanning electron micrograph (SEM) of GaN ring structure; scalebar = 2 μm. (b) Far-field CCD image of laser mode interference after scattering from end-facets of the ring shown in (a). (c) Comparison of lasing mode structure (black) and photoluminescence (blue) from a ring resonator with a partially detached facet-couple. Lasing preferentially occurs in one of the two counter-propagating resonator modes. Inset: SEM micrograph of ring; scale bar = 2 μm. (d) 0.08 s single-shot acquired spectrum for a single nanowire cavity before [dark (blue online)] and after [light (red online)] it has been shaped into a ring.

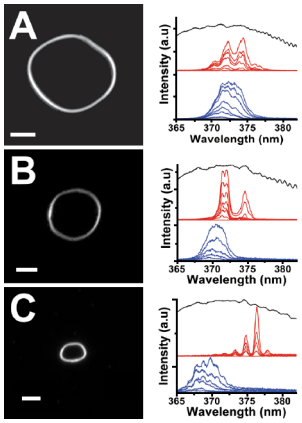

FIG. 4 (color online). (a), (b), (c) Lasing mode structure as a single nanowire cavity is sequentially cut to form progressively smaller ring diameters of 16, 12.5, and 6 μm, respectively. At right: Spontaneous emission (black trace), ring lasing [light gray trace (red online)], and uncoupled-cavity lasing [dark gray trace (blue online)] spectra for each sequential cut of the cavity. Maximum spectral emission for each ring is collected at roughly 800 μJ/cm^2, illustrating a redshift of mode position and increased mode spacing with decreasing ring diameter. All scale bars are 5 μm.

[right side of Figs. 4(a)–4(c)] after using the manipulator to cut and rejoin the end facets. It is apparent that the uncoupled peak-lasing maximum progressively shifts to higher energies. Since the gain threshold ($G_{\text{th}} = \alpha - \frac{1}{2L} \times \log[r^2]$, $\alpha =$ intrinsic cavity loss) is inversely proportional to cavity length, decreasing the cavity length can increase the gain threshold by a factor of 2 or more. Consequently, only the modes with the lowest cavity losses and highest t_c (i.e., shorter wavelength modes) will experience gain.

More interestingly, as the ring diameter is decreased the lasing modes show a progressive shift towards longer wavelengths as well as an increase in mode spacing [Eq. (1)], without showing a shift in spontaneous emission. In the smallest ring ($D \sim 6$ μm), there is emission from a mode at 378 nm (3.28 eV) which is redshifted by more than 10 meV from the next nearest cavity lasing energy. The observed redshift in these ring-resonator cavities cannot be explained by a simplified Fabry-Perot loss argument, but instead requires an understanding of the tangential, side-by-side resonator junction.

The intensity of the optical electromagnetic field is known to decay exponentially from the waveguide surface with $I(z) \propto \exp(-\frac{z}{d_p})$ [15] where d_p is a characteristic constant called the penetration depth, given by

$$d_p = \frac{\lambda}{4\pi n_w(\lambda)[\sin^2(\theta) - (\frac{1}{n_w(\lambda)})^2]^{1/2}}. \quad (2)$$

In this expression λ is the free-space wavelength, $n_w(\lambda)$ is the dispersion-corrected phase-index, and θ is the angle of incidence within the waveguide. Using a Sellmeier dispersion relation for the index [19], it is possible to compare penetration depths for characteristic lasing wavelengths from both wire (~ 370 nm) and ring (~ 380 nm) cavities. Near the critical angle for total internal reflection, the penetration depths for 370 and 380 nm light are calculated to be 66 nm and 108 nm, respectively. At a distance of 50 nm from the surface of one end facet, corresponding to the center of the adjacent tangential facet, the field intensity for the a mode at 380 nm is 30% larger than for a mode at 370 nm. Also, classical Rayleigh scattering is proportional to $\frac{1}{\lambda^4}$, implying that scattering losses will be reduced by approximately 10% for 380 nm light relative to 370 nm wavelengths. These are appreciable differences for cavities with diameters less than 150 nm, suggesting that longer wavelengths will experience better coupling (less scattering), higher quality factors ($Q = 2\pi\nu t_c$), and more gain across the tangential-facet junction.

Conclusion.—In summary, we have demonstrated significant changes in nanowire PL, Q factor, and lasing mode structure by manipulating a linear nanowire into a ring geometry. Following the side-by-side coupling of nanowire ends, peak emission wavelengths shift by nearly 10 nm due to improved coupling efficiency between tangentially overlapping nanowire ends, Q factor enhancement, and preferential gain in long-wavelength modes. These results demonstrate the versatility of nanowire laser cavities and highlight the potential of using these materials as tunable laser systems in future integrated-photonic platforms.

This work was supported by the DOE and DARPA-UPR. P. J. P. thanks the NSF for financial support. The authors thank A. Maslov and C. Z. Ning of the NASA Ames research center for helpful discussion.

*To whom correspondence should be addressed.
Email address: p_yang@berkeley.edu

[1] D. J. Sirbuly, M. Law, P. Pauzauskie, H. Q. Yan, A. V. Maslov, K. Knutsen, C. Z. Ning, R. J. Saykally, and P. D. Yang, Proc. Natl. Acad. Sci. U.S.A. **102**, 7800 (2005).
[2] P. J. Pauzauskie, T. Kuykendall, Y. F. Zhang, J. Goldberger, D. Sirbuly, J. Denlinger, and P. D. Yang, Nat. Mater. **3**, 524 (2004).
[3] J. C. Johnson, H. J. Choi, K. P. Knutsen, R. D. Schaller, P. D. Yang, and R. J. Saykally, Nat. Mater. **1**, 106 (2002).
[4] J. Goldberger, R. He, Y. Zhang, S. Lee, H. Yan, H.-J. Choi, and P. Yang, Nature (London) **422**, 599 (2003).
[5] H. J. Choi, J. C. Johnson, R. R. He, S. K. Lee, F. Kim, P. Pauzauskie, J. Goldberger, R. J. Saykally, and P. D. Yang, J. Phys. Chem. B **107**, 8721 (2003).
[6] D. J. Sirbuly, M. Law, H. Q. Yan, and P. D. Yang, J. Phys. Chem. B **109**, 15 190 (2005).
[7] A. V. Maslov and C. Z. Ning, IEEE J. Quantum Electron. **40**, 1389 (2004).
[8] Z. Y. Li and K. M. Ho, Phys. Rev. B **71**, 045315 (2005).
[9] K. J. Vahala, Nature (London) **424**, 839 (2003).
[10] M. Bayer, T. Gutbrod, J. P. Reithmaier, A. Forchel, T. L. Reinecke, P. A. Knipp, A. A. Dremin, and V. D. Kulakovskii, Phys. Rev. Lett. **81**, 2582 (1998).
[11] D. K. Armani, T. J. Kippenberg, S. M. Spillane, and K. J. Vahala, Nature (London) **421**, 925 (2003).
[12] V. R. Almeida, C. A. Barrios, R. R. Panepucci, and M. Lipson, Nature (London) **431**, 1081 (2004).
[13] M. T. Hill, H. J. S. Dorren, T. de Vries, X. J. M. Leijtens, J. H. den Besten, B. Smalbrugge, Y. S. Oei, H. Binsma, G. D. Khoe, and M. K. Smit, Nature (London) **432**, 206 (2004).
[14] D. J. Sirbuly, M. Law, J. C. Johnson, J. Goldberger, R. J. Saykally, and P. D. Yang, Science **305**, 1269 (2004).
[15] J. Jackson, *Classical Electrodynamics* (John Wiley & Sons, New York, 1999), ISBN , 3rd ed..
[16] B. E. Little, S. T. Chu, H. A. Haus, J. Foresi, and J. P. Laine, J. Lightwave Technol. **15**, 998 (1997).
[17] B. E. Little, S. T. Chu, and H. A. Haus, Opt. Lett. **23**, 1570 (1998).
[18] P. Y. Bourgeois and V. Giordano, IEEE Trans. Microwave Theory Tech. **53**, 3185 (2005).
[19] G. Yu, G. Wang, H. Ishikawa, M. Umeno, T. Soga, T. Egawa, J. Watanabe, and T. Jimbo, Appl. Phys. Lett. **70**, 3209 (1997).
[20] S. L. McCall, A. F. J. Levi, R. E. Slusher, S. J. Pearton, and R. A. Logan, Appl. Phys. Lett. **60**, 289 (1992).
[21] A. V. Maslov and C. Z. Ning, Appl. Phys. Lett. **83**, 1237 (2003).
[22] S. Gradecak, F. Qian, Y. Li, H.-G. Park, and C. M. Lieber, Appl. Phys. Lett. **87**, 173111 (2005).